Splenic T follicular helper cells compromise *Mycobacterium tuberculosis* clearance in aged C57BL/6 mice

Falak Pahwa[1], Shweta Chaudhary[1], Shivam Chaturvedi[2], Ranjan Kumar Nanda[1*]

[1]Translational Health Group, International Centre for Genetic Engineering and Biotechnology, New Delhi-110067, India

[2]Animal House, International Centre for Genetic Engineering and Biotechnology, New Delhi-110067, India

***Corresponding author:**
Ranjan Kumar Nanda (Ph.D.)
Translational Health Group, International Centre for Genetic Engineering and Technology, New Delhi-110067, India
Telephone: 91-11-26741358
Fax: 91-11-26742316
Email: ranjan@icgeb.res.in

Abstract

Ageing increases susceptibility to infectious diseases including tuberculosis. Limited literature is available on the perturbed cellular details in aged (>60 years) TB patients and understanding their molecular pathways is critical. In this study, C57BL/6 mice of multiple age groups; 2, 5, 9, 17 months (M), were aerosol infected with 100-120 colony forming unit (cfu) of *Mycobacterium tuberculosis* (Mtb) H37Rv and treated with rifampicin and isoniazid. Tissue (lungs, spleen, and liver) bacterial burden were monitored by cfu assay, liver micronutrients profiled using mass spectrometry, and tissue immune cell phenotyping was carried out employing flow cytometry. Interestingly, at 6 weeks post infection (w.p.i.), older mice (5, 9, 17M) showed similar tissue mycobacterial loads as compared to younger ones (2M). However, a delayed lung mycobacterial clearance was observed at 2 weeks post treatment in a subset of aged (17M) mice. Mtb infection led to decreased liver Fe, Zn and Se levels in 2M mice with minimum variations in 17M mice. Healthy 17M mice had higher frequency of splenic $CD4^+CD44^+CXCR5^+$, $CD4^+CD44^+PD1^+$, $CD4^+CXCR5^+PD1^+$ and T-follicular helper (TFH; $CD4^+CD44^+CXCR5^+PD1^+$) cells. Aged C57BL/6 mice showed a significant decline in the frequency of $CD4^+CD44^+CXCR5^+$ cells with infection progression, which might be contributing to the delayed Mtb clearance. Further characterization of TFH cell subsets, after careful validation, may provide insights for adjunct therapeutic development for benefitting the aged TB patients.

Keywords: TFH cells, Ageing, Immunosenescence, Tuberculosis, T cells

Introduction

Recent WHO report suggests that one in six people in the world will be aged >60 years by 2030[1]. In these aged population, immunosenescence compromises their immune competence which reduces vaccine efficacy as well as increases susceptibility to various diseases[2,4]. Overall, the geriatric population represents a large reservoir of tuberculosis (TB), caused by *Mycobacterium tuberculosis* (Mtb) infection, and have high mortality and relapse rate[3,4]. Since aged TB patients show atypical presentation irrespective of the settings (i.e. developed or developing world), strategies that might improve the compromised immune system will positively influence the disease management.

Animal models (C57BL/6, BALB/c, C3HeB/FeJ) of 6-8 weeks age (which is equivalent to human of 18-20 years[5]) are commonly used to delineate TB pathophysiology. $B6D2F_1$ mice of 24 months (M) infected with Mtb H37Rv strain showed initial resistance but succumbed to the infection by 8 weeks[6,7]. This is attributed to a higher $CD8^+$ T cell frequency and delayed antigen-specific $CD4^+$ T cell responses[8,9]. T-follicular helper (TFH) cells expand during infection and accumulation of $CD4^+CXCR5^+$ T cells in the lungs of Mtb infected C57BL/6 mice has been reported[10,11]. Ageing induces TFH cell dysfunction and impairs its differentiation by IL-10 and IFN-γ production, further reducing the host response against invading pathogens[12]. Immune cell profiling of Mtb infected mice representing human equivalence age of adult and geriatric population might be useful to identify important cell subtypes for further targeting their dysfunctional pathways.

In this study, C57BL/6 mice of multiple age groups (human equivalence in years)[5]: 2M (18-20), 5M (28-30), 9M (35-38), and 17M (56-60) were infected with low aerosol dose of Mtb to monitor their tissue bacterial burden and immune cell frequencies. The lung Mtb load of various age groups were similar till 6 weeks post infection (w.p.i.). However, a delay in the lung mycobacterial clearance was observed in 17M mice post 2 weeks of rifampicin (RIF) and isoniazid (INH) treatment (w.p.t.) compared to 2M group. Higher splenic TFH ($CD4^+CD44^+CXCR5^+PD1^+$) frequency was observed in 17M old control and Mtb infected mice compared to 2M groups. At 6 w.p.i., TFH cell frequency declines in Mtb infected 17M mice compared to healthy controls. The delayed Mtb clearance observed in the lungs of aged mice could be attributed to the altered TFH cell frequency and function. Functional characterization of the TFH cell subsets could be important to identify targets for developing adjunct therapeutics for aged TB patients.

Materials and methods

Experimental groups, Mtb infection and treatment: Procedures adopted in this study were performed following the recommended Guidelines for Care and Use of Laboratory Animals and approved by the Animal Ethics Committee of ICGEB, New Delhi (Ref No. ICGEB/IAEC/07032020/TH-10). C57BL/6 mice of multiple age groups (female: 2/5/9M; male: 2/17M) were procured from ICGEB animal house and transferred to Tuberculosis Aerosol Challenge Facility (TACF; BSL-3 facility). Mice were fed chow diet and water ad libitum throughout the experiments and maintained at 20-22 °C; 45-60 % humidity with 12 h light/dark cycle. Weight adjusted and randomly grouped mice (n=4/5 per group) were used in the experiments. After 1 week of conditioning in TACF, mice were infected with a low dose of animal passaged H37Rv strain (100-120 colony forming unit; cfu) in Madison aerosol exposure chamber (University of Wisconsin, USA). Phthiocerol dimycocerosates (PDIM) levels of H37Rv strain used for infection were monitored by thin layer chromatography following an earlier report (**Supplementary Figure S1**)[13]. Body weight of mice was recorded at multiple time points (pre-infection, 2, 4 and 6 w.p.i. and post treatment) during the experiments. After 2 w.p.i., a subset of mice was treated with RIF (100 mg/L) and INH (100 mg/L) in drinking water and were replaced with fresh drug solutions at every 48 hours. A single mouse belonging to 17M group died before completion of 4 w.p.t. and abscess bearing mouse was excluded from the study. Under isoflurane anaesthesia, mice were sacrificed and tissues (lung, spleen, and liver) were harvested for bacterial cfu assay and immune cells were isolated at indicated time points. A part of the tissue was kept in neutral buffered formalin (500 µL, 10 %) for histology analysis. A part of liver sample was rinsed with chilled PBS and after putting it in liquid nitrogen, were stored in -80 °C for subsequent micronutrient profiling using inductive coupled plasma mass spectrometry (ICP-MS).

Bacterial load monitoring by cfu assay: Briefly, the organs (left lobe of lungs, half of spleen, and two third of liver) were homogenized using T-25 digital Ultra-Turrax disperser (IKA, India) in phosphate buffered saline (1 mL). The homogenates were serially diluted and plated in duplicates on 7H11 agar supplemented with Middlebrook OADC (10%, BD Biosciences, #211886). These plates were incubated at 37 °C in a humidified incubator and bacterial colonies were enumerated at 3 weeks post inoculation.

Histology: Formalin fixed tissues were paraffin embedded and sectioned using a sliding microtome (Thermo Scientific, USA). Tissue sections (100 µm) were stained with Hematoxylin and Eosin (H&E) and analysed under a light microscope (Nikon, at 100/400 ×

magnification). Individual slides without the group information were shared with the pathologist for scoring to minimise the bias.

Liver micronutrient profiling: Liver samples (100 mg) of C57BL/6 mice (2M and 17M) of healthy, Mtb infected and drug treated groups were subjected to microwave digestion. A mixture of HNO_3 (Sigma, USA) and H_2O_2 (Supelco, 30% Suprapur) were used for digestion following the parameters: 150W for 10 min, held for 15 min, 250W for 10 min and held for 15 min in a multiwave-pro digestor (Anton Paar, USA). Double distilled water (Barnstead™ Smart2Pure water purification system, Thermo Scientific, USA) was used to dilute the digested liver samples and introduced to ICP-MS (Thermo Scientific iCAP-TQ, USA) in kinetic energy discrimination (KED) mode using argon as carrier. ICP-MS data acquisition was carried out using Qtegra software (version: 2.10.4345.39) to monitor ^{57}Fe, ^{63}Cu, ^{66}Zn and ^{77}Se. Using standard curves of micronutrients (range 1-1000 ppb), the absolute amount of liver micronutrients was calculated for comparative analysis between the study groups.

Immune cell isolation: Harvested tissues (right lobe of lungs/half spleen) of each mouse belonging to 2M/17M age groups were incubated with collagenase D (1 µg/mL, Sigma, #11088866001) and DNase I (0.5 mg/mL, Sigma, #10104159001) in RPMI media 1640 (Gibco, #31800022) at 37 °C for 30 min. The cell suspension was passed through a cell strainer (70 µm) and centrifuged at 400 × g at 4 °C for 5 min. The cell pellet was lysed with RBC cell lysis buffer (ACK buffer, filter sterilized) at room temperature for 5 min. After washing the immune cells with PBS, cell surface staining was carried out. Because of low yield, immune cell isolation of lungs of healthy mice (2M and 17M) was not attempted in this study. Lungs of Mtb infected mice receiving RIF and INH also had low cell numbers and excluded from this study.

Immune cell profiling: Harvested lungs and spleen immune cells were incubated with recommended dilutions of antibodies (BioLegend, USA) conjugated to fluorophores: CD3-BV510 (#100234), CD4-BV785 (#100552), CD8-Alexa fluor 700 (#100730), CD44-BV605 (#103047), CXCR5-PE/Dazzle (#145522), PD1-PE-Cy7 (#109110) and KLRG1-BV421 (#138414) on ice for 45 min. After washing with buffer (0.2 % FBS in 1× PBS) twice, cells were fixed with fixation buffer (1×, #005123, eBioscience). Flow cytometry data were acquired using BD LSRFortressa X-20 (BD Biosciences, USA). A minimum of 1 million events was acquired per sample. The acquired flow cytometry data were analysed using FCS Express (DeNovo software, version 6).

Statistical Analysis: The body weight, cfu, micronutrients, immune cell frequency data were analyzed by parametric analysis using Student's t-test in GraphPad Prism version 8.4.2 (GraphPad Software, San Diego, CA). All data are presented as mean ± standard deviation (S.D.). A p-value of ≤0.05 were treated as significant at 95% confidence interval. Information about the sample size and statistical analysis adopted in each experiment have been provided in the individual figure legend.

Results

Mid-aged C57BL/6 mice (9M, female) showed early Mtb dissemination: The steps adopted for this experiment are highlighted in **Figure 1A**. Older (9 and 5M) mice had significantly higher body weight than the control group (2M) (**Figure 1B**). The body weight gain observed in the healthy mice showed a marginal decline in Mtb infected group with major changes in 5M mice (p=0.03) (**Figure 1C**, **Supplementary Figure S2**). Irrespective of their age, infection and treatment status, the gross morphology of multiple tissues (lung, spleen, and liver) was similar (**Figure 1D**, **Supplementary Figure S3**, **S4**). The lung histopathological scores depicted a time dependent increase in pathology with multiple foci of infiltrating cells and granulomatous lesions in the Mtb infected mice groups (**Figure 1E**, **Supplementary Figure S5**). Lung pathologies of mice receiving treatment were significantly resolved by 4 w.p.t. (**Figure 1E**). Interestingly, liver of Mtb infected mice of all age groups showed mild degenerative changes, which partially resolved upon treatment (**Figure 1F**, **Supplementary Figure S5**). Lung mycobacterial burden increased from 2 to 6 w.p.i. in all the age groups (**Figure 1G**). Interestingly, at the early time point (2 w.p.i.), spleen of 9M and liver of 5M mice showed significantly higher mycobacterial burden with respect to the 2M controls (**Figure 1H**, **1I**). However, the lung mycobacterial burden was comparable between the age groups at both 2 and 6 w.p.i.. At later time point i.e. 6 w.p.i., the spleen and liver Mtb burden was similar in all study groups **(Figure 1H**, **1I)**. Infected mice of all the age groups after 4 w.p.t. had significant (~2.5 log) reduction in the Mtb burden in lungs, spleen, and liver (**Figure 1G**, **1H**, **1I**).

Aged C57BL/6 mice (17M, male) showed compromised lung Mtb clearance: The experimental details used in this study are presented in **Figure 2A**. Aged C57BL/6 (17M) mice had significantly higher (1.23×, p<0.0001) body weight than 2M mice before infection (**Figure 2B**). Mtb infection induced body weight changes were different in both the age groups wherein 17M mice lost higher body weight (-6 % Δ body weight, **Figure 2C**, **Supplementary Figure**

S6) compared to 2M control mice. The gross morphology of lung, spleen and liver were found to be similar in Mtb infected 2M and 17M mice (**Figure 2D**, **Supplementary Figure S7**, **S8**, **S9)**. Mtb infected lungs showed multiple foci of infiltrating cells and granulomatous lesions with a maximum histopathological score at 6 w.p.i. which resolved within 4 w.p.t. (**Figure 2E**, **Supplementary Figure S10**). Spatio temporal adaptation of Mtb in the liver of 2M and 17M mice resulted in mild degeneration, which was restored within 2 w.p.t. (**Figure 2F**). Tissue Mtb burden in the lungs, spleen, and liver of both 2M and 17M mice peaked by 4 w.p.i. and remained similar till 6 w.p.i. (**Figure 2G**, **2H**, **2I**). In the early treatment period, i.e. 2 w.p.t., a compromised lung mycobacterial clearance was observed in 17M group (two out of five mice showed ~3 $\log_{10}$ cfu compared to ~1.2 $\log_{10}$ cfu in 2M, **Figure 2G**). However, the spleen and liver mycobacterial loads in both the age groups were below the limit of detection (LOD) (**Figure 2H**, **2I**). At later time point i.e. 4 w.p.t. completion, the lung Mtb load of both age groups were below the LOD (**Figure 2G**).

Deregulated micronutrient balancing observed in Mtb infected aged mice: Liver of 17M mice showed significantly lower levels of Zn (17M/2M=0.14×, $p<0.0001$) and higher Cu (4.28×, $p<0.0001$) compared to 2M mice. However, both age groups had similar Fe (0.99×, $p=0.98$) and Se (0.77×, $p=0.08$) levels (**Figure 2J**). Upon Mtb infection, hepatic Fe ($p=0.05$), Zn ($p=0.04$) and Se ($p=0.05$) levels were found be lower in 2M mice at 4 w.p.i. but such changes were absent in 17M mice compared to healthy controls (**Figure 2J**). Interestingly, RIF and INH treatment for 2 weeks reversed the hepatic Zn ($p=0.02$) and Se ($p=0.03$) levels in 2M mice. Whereas, 17M mice treated mice showed higher Fe ($p=0.04$) and Cu ($p<0.0001$) levels with lower Zn ($p<0.0001$) compared to 2M mice (**Figure 2J**).

$CD4^+CD44^+KLRG1^+PD1^+$ cells of Mtb infected lungs in aged mice showed decline by 6 w.p.i.: Immune cells harvested from the lungs of 2M and 17M mice were profiled using flow cytometry with the following gating strategy (**Figure 3A**, **3B**, **3C**). At early time point, i.e. 4 w.p.i., the total lung $CD4^+$ T cells were similar between Mtb infected 2M and 17M groups. Although, significant increase in $CD4^+$ T cells was observed by 6 w.p.i. in both the groups, 17M mice had lower (17M/2M=0.74×, $p=0.02$) frequency compared to the younger group (**Figure 3D**). Activated $CD4^+$ T cells ($CD4^+CD44^+$) were higher at 4 w.p.i. in 17M mice compared to 2M (17M/2M=1.64×, $p=0.03$) but with infection progression, at 6 w.p.i., 2M mice showed significantly ($p=0.05$) higher number of activated cells (**Figure 3E**). $CD4^+CXCR5^+$ T cell frequency increased from 4 to 6 w.p.i. in both 2M and 17M mice (**Figure 3F**). We also

observed higher proportion (1.93×, p=0.05) of $CD4^+CD44^+CXCR5^+$ T cells at 6 w.p.i. in 17M mice than 2M ones (**Figure 3G**). Expression of PD1 and KLRG1 on $CD4^+$ T cells and activated $CD4^+$ T cells remained similar at 4 and 6 w.p.i. in both the age groups (**Figure 3H**, **3I**, **3J**, **3K**). The abundance of $CD4^+CXCR5^+PD1^+$ cells increased at 6 w.p.i. in mice of both the age groups (**Figure 3L**). In 2M mice, $CD4^+CD44^+KLRG1^+PD1^+$ cells remained similar at both the time points, whereas it declined significantly (p<0.0001) in 17M mice by 6 w.p.i. (**Figure 3M**).

Splenic TFH cell frequency decreased in Mtb infected aged mice: Splenocytes of 2M and 17M mice were processed and profiled using flow cytometry following the gating strategy presented (**Figure 4A**, **4B**, **4C**). Total splenic $CD4^+$ T cell population in 2M and 17M mice remained similar upon Mtb infection at both the time points (**Figure 4D**). Splenic $CD4^+CD44^+$ cells remain unchanged in Mtb infected 2M mice throughout the experiment but decreased by 6 w.p.i. in 17M mice (**Figure 4E**). $CD4^+CXCR5^+$ T cells increased as infection progressed in both the age groups (**Figure 4F**). Interestingly, at 6 w.p.i., $CD4^+CD44^+CXCR5^+$ T cells increased in infected 2M mice while decreased in 17M mice compared to 4 w.p.i. (**Figure 4G**). Similar frequencies of $CD4^+PD1^+$, $CD4^+KLRG1^+$, $CD4^+CD44^+PD1^+$, and $CD4^+CD44^+KLRG1^+$ cells were observed at both the time points of Mtb infected 2M and17M mice, however 17M mice showed increased PD1 expression as compared to 2M mice (**Figure 4H**, **4I**, **4J**, **4K**). $CD4^+CXCR5^+PD1^+$ T cell frequency was higher in infected 2M and 17M mice and showed a time dependent increase, with 17M mice having an overall higher abundance than 2M mice (**Figure 4L**). $CD4^+CD44^+CXCR5^+$ $PD1^+$ cell frequency did not change in 2M mice as infection progressed whereas 17M mice showed a decrease in frequency by 6 w.p.i. (**Figure 4M**). At 4 w.p.i., $CD4^+CD44^+KLRG1^+PD1^+$ cells were significantly low in 2M mice than 17M group but this difference was lost by 6 w.p.i. (**Figure 4N**). While, $CD4^+CD44^+KLRG1^+PD1^+$ cell frequency showed a time dependent decrease from 4 to 6 w.p.i. in 17M mice (**Figure 4N**).

Splenic $CD4^+$ T cells of healthy 17M mice was lower with an increase in frequency of $CD4^+CXCR5^+$, $CD4^+PD1^+$, $CD4^+CXCR5^+PD1^+$, $CD4^+CD44^+$, $CD4^+CD44^+CXCR5^+$, $CD4^+CD44^+PD1^+$, and $CD4^+CD44^+CXCR5^+$ $PD1^+$ cells than 2M controls (**Supplementary Figure S11**). However, KLRG1 expression remained similar on total and activated $CD4^+$ T cells of both 2M and 17M groups (**Supplementary Figure S11**). Post 4 weeks of RIF and INH treatment, 17M mice had higher splenic $CD4^+CD44^+$, $CD4^+CXCR5^+$, $CD4^+CD44^+CXCR5^+$, $CD4^+PD1^+$, $CD4^+CD44^+PD1^+$ cell frequency, with decreased

$CD4^+CXCR5^+PD1^+$ cells (**Supplementary Figure S12**). KLRG1 expression was higher in 17M treated mice at 2 w.p.t. as compared to 2M mice (**Supplementary Figure S12**).

Discussion

Overall global population distribution is shifting towards aged (>60 years) groups, which will also influence the total aged TB patient population. Several seminal studies have demonstrated that molecular and physiological changes accumulate with ageing in organs including the lungs and immune system, making aged subjects more susceptible to TB[14]. Ageing-associated decline in innate and adaptive immune responses result in immunosenescence with detrimental alteration in cellular functions, and interactions of lung resident cells with systemic immune cells[15,16]. To understand TB pathophysiology, inbred mouse strains (C57BL/6, BALB/c, C3HeB/FeJ) with varied Mtb susceptibility are commonly used[17]. However, except few, majority of the studies have focused on 6-8 weeks old animals that corresponds to 18-20 years aged human[5]. So, understanding Mtb infection-associated perturbations in aged animals might provide useful cellular and molecular details to develop strategies for validation in aged TB patients for a better clinical management.

Cachexia is a common characteristic feature of majority of the newly diagnosed or relapsed TB patients, which partially recovers upon treatment completion[18]. Younger (2M) mice infected with Mtb lost ~6% body weight within 4 w.p.i. and ~3% in aged (17M) mice as compared to their healthy controls. The lost body weight in infected mice was regained within 4 w.p.t. and reached to a comparable weight to the healthy counterparts. An earlier report showed ~25% body weight loss by ~3 w.p.i. in C3H animals[19]. Weight loss patterns observed in animal models infected with Mtb may vary based on the bacterial virulence status, dose, route of infection, animal strain and time points adopted in the studies[20].

The lung mycobacterial load showed a time dependent increase as infection progressed up to 6 w.p.i. in all the age groups (female; 2M, 5M, and 9M C57BL/6) which corroborates with an earlier report[21]. However, in 9M mice, we observed a significantly higher spleen Mtb load at 2 w.p.i. as compared to the younger group (2M). It is suggestive of an early initiation of immunity[22], thus contributing to an advantage of mid-aged animals above younger animals (~2M) to mount a quick and robust immune response post infection. An earlier report showed similar course of infection in lungs, spleen, and liver of 3M and 12M $AB6F_1$ female mice infected with Mtb through intravenous (i.v.) route[6]. In BALB/c mice, Mtb dissemination to extra-pulmonary sites such as spleen and liver, was observed by 2 weeks post intratracheal

introduction[23]. Within 4 w.p.t., lung mycobacterial loads of 2M, 5M and 9M animals were below the LOD. Similar observation was reported in 2M female C57BL/6 mice treated with RIF (300 mg/L) and INH (600 mg/L) within 2 w.p.t.[24]. As the tissue cfu were similar between age groups (2M, 5M and 9M) and time points (2 and 6 w.p.i.), an additional time point (4 w.p.i./2 w.p.t.) was added in the experiment including extreme age groups (2M and 17M). Male C57BL/6 mice are reported to be more susceptible to Mtb infection with higher mycobacterial loads, accelerated disease progression and premature death compared to females[25]. Also, the prevalence of TB in males was reported to be four times higher than females[26]. Therefore, we selected two extreme age groups of male C57BL/6 mice in the next experiment.

Up to 6 w.p.i., 17M C57BL/6 mice had similar tissue (lung, spleen, and liver) Mtb load as 2M groups. Young and older mice, irrespective of the route of infection via aerosol or i.v., control Mtb proliferation initially (by ~8 w.p.i.)[6,7]. This control of infection is reported to be gradually lost in older mice (18M) compared to young mice[27,28]. Male C57BL/6 mice of 3M and 18M age groups infected with Mtb (100-200 cfu) showed low lung bacterial load at 4 w.p.i. but increased significantly by 8 w.p.i. in 18M animals[29]. $B62DF_1$ mice (24M) infected with 50 cfu of Mtb showed similar lung bacterial load as 2M animals up to ~11 w.p.i.[7]. Aged (>20M) mice showed higher lethality upon infections with *Listeria monocytogenes*, *Salmonella typhimurium*, and *Toxoplasma gondii*[30]. In this study, the hematogenous spread of infection from lungs to the liver were similar between 2M and 17M mice whereas a higher spread was reported in 24M $B62DF_1$ mice[7]. Female C57BL/6 mice (18M) had lower lung Mtb burden at 2 w.p.i. with respect to the younger 3M mice[9]. These mixed observations about age-associated changes in tissue Mtb load reported by multiple authors including us, could be majorly attributed to the route of infection, bacterial dose, gender, and genetics of the host and pathogen.

Trace metals are reported to play a role in the decline of systemic immune responses and modulation of the redox status in aged host[31]. Low circulatory Zn and Fe levels in TB patients are reported and that contributes to an impaired lymphocyte development, polarization into effector cells, and their functions[32-34]. Observed increase in liver Cu/Zn and declined Fe/Cu ratios in aged mice, might partially contribute to the weakened Mtb clearance. Alteration in liver function in aged animals is known to influence drug metabolism and Mtb clearance[35].

Aged animals show a perturbed $CD4^+$ T cell-mediated immunity with altered frequency and compromised function leading to a poor response of antigen-specific $CD4^+$ T cells[27,36]. $AB6F_1$ mice (24M) succumbed within 8 weeks to Mtb infection (10^5 cfu, i.v.) but younger mice (2M) survived till 4 months[6]. A mathematical model predicted lower lung Mtb load by 3 w.p.i.

in 18M mice which gradually exceeds the load in 3M mice by 6 w.p.i., partially due to a delayed $CD4^+$ T cell response[37,38]. Diminished IL-12 response, which drives IFN-γ production, leads to a delayed emergence of $CD4^+$ T cells in the aged animals[7,37]. Furthermore, these $CD4^+$ T cells in aged mice showed a poor expression of L-selectin and CD11a, which are important for T cell movement across inflamed endothelial blood vessel surfaces[37]. To compensate for the delayed influx of $CD4^+$ T cells into the lungs, older mice rely on CD8-mediated immune responses[26]. Interestingly, older $AB6F_1$ mice (19-30M) were able to generate enough protective T cells against *Listeria monocytogenes*[39].

At 2 w.p.t., 17M C57BL/6 mice had higher lung Mtb load (~2 $\log_{10}$) compared to younger mice (2M), suggesting a delayed mycobacterial clearance. The observed lung Mtb clearance in 2M mice completing 2 w.p.t. corroborates with earlier reports[24,40-42]. Limited literature information on aged mice treated with anti-TB drugs and their effect on T cell repertoire and mycobacterial clearance kinetics is available. Therefore, we monitored the markers for T cell activation (CD44), late-stage memory (PD1, KLRG1) and homing receptor CXCR5 in the immune cells harvested from the lungs and spleen of 2M and 17M age groups to correlate the delayed lung Mtb clearance in aged mice. At the later time point (6 w.p.i.), aged mice had lower lung $CD4^+$ T cells frequency than younger mice corroborating earlier report[6]. Aged Mtb infected mice had higher lung $CD4^+CD44^+KLRG1^+PD1^+$ and $CD4^+CD44^+CXCR5^+$ cells than the younger group at 4 and 6 w.p.i. respectively. In 2M and 17M mice groups, after 4 w.p.i. significantly higher lung $CD4^+CXCR5^+$, $CD4^+CD44^+CXCR5^+$ and $CD4^+CXCR5^+PD1^+$ cell frequencies were observed. The accumulation of activated $CD4^+CXCR5^+$ T cells, that produce pro-inflammatory cytokines, in the Mtb infected lungs of 2M B6 mice was reported[11]. Splenic $CD4^+$ T cell frequency of healthy 17M mice was lower with an increased expression of CXCR5 and PD1 on total and activated $CD4^+$ T cells than 2M controls. Upon Mtb infection, the splenic $CD4^+$ T cell count were similar between 2M and 17M groups at both 4 and 6 w.p.i., corroborating with earlier report on infected C57BL/10 mice of multiple age groups (3, 6, 12, 24M)[43]. Higher splenic $CD4^+CD44^+$, $CD4^+CXCR5^+$, $CD4^+PD1^+$ and $CD4^+CD44^+PD1^+$ cell frequencies in 17M mice were observed at both time points compared to 2M controls. Mtb infected aged mice had higher splenic $CD4^+CXCR5^+PD1^+$ cells but a decline in $CD4^+CD44^+CXCR5^+$ cells was observed at 6 w.p.i. as compared to healthy controls. At 4 w.p.t., 17M mice showed similar $CD4^+CXCR5^+$ cell frequency, with decreased $CD4^+CXCR5^+PD1^+$ cells, suggesting the inability of the host to elicit proper TFH response. Irrespective of infection and treatment status, higher PD1 expression was observed in the splenic T cells of 17M mice, which also suppress TFH development[44]. Compromised Mtb clearance in aged mice might be due to the impaired

TFH cell functionality as reported earlier[45] (**Figure 5**). TFHs link the humoral and antibody mediated immunity by driving antibody induction during various infections[46]. Low TFH cell frequency with higher expression of inhibitory receptors like Tim-3 and PD-1 was reported in TB patients[47]. Blockade of Tim-3 and PD-1 with monoclonal antibodies restored TFH cell frequency and function ex-vivo[47]. Mtb antigen induced TFH cell frequency was significantly lower in pulmonary TB patients compared to latent TB subjects with a lower IL-21 expression[48]. Higher circulating TFH cell frequency was reported in other disease conditions like systemic lupus erythematosus, Sjögren's syndrome, sarcoidosis and malaria[49,50]. Understanding the molecular mechanism that contributes to the alteration in frequency or impaired function of TFH cell subsets might identify critical targets for alleviating the immune dysfunction in the aged host.

Higher splenic $CD4^+CD44^+KLRG1^+PD1^+$ cells were observed in 17M Mtb infected mice at 4 w.p.i. compared to the younger (2M) mice. Expression of KLRG1 and PD-1 was marginally increased on $CD4^+$ T-cells in active TB patients, compared to healthy donors[51]. The frequency of these cells was higher in aged mice at 2 w.p.t., which is also reported in TB patients completing treatment[51]. In mice model receiving RIF and INH, reduced KLRG1-expression on $CD4^+$ and $CD8^+$ T cells was reported[52]. KLRG1 is a T cell differentiation indicator in murine TB, and the higher KLRG1 expression observed in aged infected mice indicates that Mtb is priming terminal differentiation of the effector memory cells, which restricts their migration to the lungs[53].

However, this study has certain limitations. Monitoring Mtb specific immune responses to the observed variation in immune cell distribution of aged and younger infected animals might provide useful information. The immune cell profiling result is from male, 2M and 17M C57BL/6 mice, however it would be interesting to capture the details in aged female mice. Immune cell phenotyping data were generated from a limited number of animals, which could be expanded in subsequent studies for further confirmation.

In this study, we report a delayed Mtb clearance from the lungs of aged (17M) mice and low splenic TFH cells, which might be due to virtue of an impaired TFH function, that needs additional investigation. Identification of important T cell subsets like TFHs cells in aged host and improving their function might be useful in developing strategies which could cater to the geriatric comorbid TB patients on which limited details are available.

Acknowledgements

FP is supported by the fellowship from Department of Biotechnology, Government of India. SC is a Shyama Prasad Mukherjee fellow and is supported by Council of Scientific and Industrial Research, Government of India. The core support from International Centre for Genetic Engineering and Biotechnology (ICGEB), New Delhi to RKN is highly acknowledged. Haripriya Priyadarsini, Adyasha Sarangi, and Hossain Md. Faruquee are acknowledged for their help and support during the animal experiments. Help from staff of animal house and Tuberculosis Aerosol Challenge Facility (TACF) at ICGEB, New Delhi is acknowledged. TACF is supported by Department of Biotechnology, Government of India. Part of these research findings were presented in World Conference on Lung Health 2022, Virtual, 8-11 November 2022 organized by The Union and 2nd biennial meeting on Sex Differences in the Immune Systems conference, virtual, 30 November- 2 December 2022 organized by Trinity College Dublin & Whitehead Institute. Figures 3B, 4B and 5 were created with Biorender.com.

Additional information

This article has supplemental information.

Competing interests

The authors declare no conflict of interest.

Author Contributions

FP and RKN conceptualized the project. RKN acquired funding, shared resources, and administrated the project. FP and SC carried out animal experiments, immune cell staining, flow cytometry data acquisition. ShiC calculated histopathological scores. FP and RKN analysed the data and wrote the original draft and updated co-authors suggestions. The manuscript was reviewed and approved by all co-authors.

References

1. https://www.who.int/news-room/fact-sheets/detail/ageing-and-health. (Accessed on 01/02/2023)
2. Castle, S. C., Uyemura, K., Fulop, T., and Makinodan, T. Host resistance and immune responses in advanced age. *Clinics in geriatric medicine* 23.3 (2007): 463-479.

3. Ledesma, J. R., et al. Global, regional, and national sex differences in the global burden of tuberculosis by HIV status, 1990-2019: Results from the global burden of disease study 2019. *The lancet infectious diseases* 22.2 (2022): 222-241.
4. Yew, W. W., Yoshiyama, T., Leung, C. C., and Chan, D. P. Epidemiological, clinical and mechanistic perspectives of tuberculosis in older people. *Respirology* 23.6 (2018): 567-575.
5. Flurkey K., Currer J.M., and Harrison D.E. The mouse in aging research. *The mouse in biomedical research 2nd edition*. American college laboratory animal medicine (Elsevier), Burlington, MA. (2007): 637-672.
6. Orme, I. M. Aging and immunity to tuberculosis: Increased susceptibility of old mice reflects a decreased capacity to generate mediator T lymphocytes. *Journal of immunology* 138.12 (1987): 4414-4418.
7. Cooper, A. M., et al. Old mice are able to control low-dose aerogenic infections with *Mycobacterium tuberculosis*. *Infection and immunity* 63.9 (1995): 3259-3265.
8. Haynes, L. et al. Interleukin 2, but not other common γ chain–binding cytokines, can reverse the defect in generation of CD4 effector T cells from naive T cells of aged mice. *The journal of experimental medicine* 190.7 (1999): 1013-1024.
9. Vesosky, B. et al. Age dependent increase in early resistance of mice to *Mycobacterium tuberculosis* is associated with an increase in CD8 T cells that are capable of antigen independent IFN-γ production. *Experimental gerontology* 41.11 (2006): 1185-1194.
10. Crotty, S. T follicular helper cell differentiation, function, and roles in disease. *Immunity* 41.4 (2014): 529-542.
11. Slight, S. R., et al. $CXCR5^+$ T helper cells mediate protective immunity against tuberculosis. *The journal of clinical investigation* 123.2 (2013): 712-726.
12. Lefebvre, J. S., Masters, A. R., Hopkins, J. W., and Haynes, L. Age-related impairment of humoral response to influenza is associated with changes in antigen specific T follicular helper cell responses. *Scientific reports* 6.1 (2016): 25051.
13. Domenech, P., and Reed, M.B. Rapid and spontaneous loss of phthiocerol dimycocerosate (PDIM) from *Mycobacterium tuberculosis* grown in vitro: Implications for virulence studies. *Microbiology (Reading, England)* 155.Pt 11 (2009): 3532-3543.
14. Lee, S., et al. Molecular programs of fibrotic change in aging human lung. *Nature communications* 12.1 (2021): 6309.
15. Nikolich-Žugich, J. The twilight of immunity: Emerging concepts in aging of the immune system. *Nature immunology* 19.1 (2018): 10-19.

16. Cho, S. J., and Stout-Delgado, H.W. Aging and lung disease. *Annual review of physiology* 82 (2020): 433-459.
17. Kramnik, I., and Beamer, G. Mouse models of human TB pathology: Roles in the analysis of necrosis and the development of host-directed therapies. *Seminars in immunopathology* 38 (2016): 221-237.
18. Bernabe-Ortiz, A., Carcamo, C. P., Sanchez, J. F., and Rios, J. Weight variation over time and its association with tuberculosis treatment outcome: A longitudinal analysis. *PLoS one* 6.4 (2011): e18474.
19. Nikonenko, B. V., Samala, R., Einck, L., and Nacy, C. A. Rapid, simple in vivo screen for new drugs active against *Mycobacterium tuberculosis*. *Antimicrobial agents and chemotherapy* 48.12 (2004): 4550-4555.
20. Dong, H., et al. Differences in pathogenicity of three animal isolates of *Mycobacterium* species in a mouse model. *PLoS one* 12.8 (2017): e0183666.
21. Rhoades, E. R., Frank, A. A., and Orme, I. M. Progression of chronic pulmonary tuberculosis in mice aerogenically infected with virulent *Mycobacterium tuberculosis*. *Tubercle and lung disease* 78.1 (1997): 57-66.
22. Chackerian, A. A., et al. Dissemination of *Mycobacterium tuberculosis* is influenced by host factors and precedes the initiation of T-cell immunity. *Infection and immunity* 70.8 (2002): 4501-4509.
23. De Steenwinkel, J. E. M., et al. Immunological parameters to define infection progression and therapy response in a well-defined tuberculosis model in mice. *International journal of immunopathology and pharmacology* 22.3 (2009): 723-734.
24. Lenaerts, A. J., et al. Significant increases in the levels of liver enzymes in mice treated with anti-tuberculosis drugs. *International journal of antimicrobial agents* 26.2 (2005): 152-158.
25. Dibbern, J., Eggers, L., and Schneider, B. E. Sex differences in the C57BL/6 model of *Mycobacterium tuberculosis* infection. *Scientific reports* 7.1 (2017): 1-8.
26. Sathiyamoorthy, R., et al. Prevalence of pulmonary tuberculosis in India: A systematic review and meta-analysis. *Lung India* 37.1 (2020): 45-52.
27. Orme, I. Mechanisms underlying the increased susceptibility of aged mice to tuberculosis. *Nutrition reviews* 53.4 (1995): S35-S40.
28. Turner, J., Frank, A. A., and Orme, I. M. Old mice express a transient early resistance to pulmonary tuberculosis that is mediated by CD8 T cells. *Infection and immunity* 70.8 (2002): 4628-4637.

29. Lafuse, W.P., et al. Psychological stress creates an immune suppressive environment in the lung that increases susceptibility of aged mice to *Mycobacterium tuberculosis* infection. *Frontiers in cellular and infection microbiology* (2022): 1372.
30. Louria D.B., Sen P., and Buse M. Age-dependent differences in outcome of infections, with special reference to experiments in mice. *Journal of the American geriatrics society* 30.12 (1982): 769-773.
31. Lossow K., et al. Aging affects sex-and organ-specific trace element profiles in mice. *Aging (Albany NY)* 12.13 (2020): 13762-13790.
32. Keflie T.S., et al. Vitamin A and zinc deficiencies among tuberculosis patients in Ethiopia. *Journal of clinical tuberculosis and other mycobacterial diseases* 12 (2018): 27-33.
33. Sargazi, A., et al. Role of essential trace elements in tuberculosis infection: A review article. *Indian journal of tuberculosis* 64.4 (2017): 246-251.
34. Honscheid A., Rink L., and Haase H. T-lymphocytes: A target for stimulatory and inhibitory effects of zinc ions. *Endocrine, metabolic & immune disorders-drug targets (formerly Current drug targets-immune, endocrine & metabolic disorders)* 9.2 (2009): 132-144.
35. Thompson, N. P., et al. Anti-tuberculosis medication and the liver: Dangers and recommendations in management. *European respiratory journal* 8.8 (1995): 1384-1388.
36. Akbar, A. N. and Fletcher, J. M. Memory T cell homeostasis and senescence during aging. *Current opinion in immunology* 17.5 (2005): 480-485.
37. Orme, I. M., Griffin, J. P., Roberts, A. D., and Ernst, D. N. Evidence for a defective accumulation of protective T cells in old mice infected with *Mycobacterium tuberculosis*. *Cellular immunology* 147.1 (1993): 222-229.
38. Friedman A., Turner J., and Szomolay B. A model on the influence of age on immunity to infection with *Mycobacterium tuberculosis*. *Experimental gerontology* 43.4 (2008): 275-285.
39. Løvik, M., and North, R. J. Effect of aging on antimicrobial immunity: Old mice display a normal capacity for generating protective T cells and immunologic memory in response to infection with *Listeria monocytogenes*. *Journal of immunology* 135.5 (1985): 3479-3486.
40. Dutta, N. K., Pinn, M.L. and Karakousis, P.C. Reduced emergence of isoniazid resistance with concurrent use of thioridazine against acute murine tuberculosis. *Antimicrobial agents and chemotherapy* 58.7 (2014): 4048-4053.

41. Vilchèze, C., Kim, J., and Jacobs Jr, W. R. Vitamin C potentiates the killing of *Mycobacterium tuberculosis* by the first-line tuberculosis drugs isoniazid and rifampin in mice. *Antimicrobial agents and chemotherapy* 62.3 (2018): e02165-17.
42. Lenaerts, A. M., Chase, S. E., Chmielewski, A. J., and Cynamon, M. H. Evaluation of rifapentine in long-term treatment regimens for tuberculosis in mice. *Antimicrobial agents and chemotherapy* 43.10 (1999): 2356-2360.
43. Turner, J., and Orme, I.M. Identification of altered integrin α/β chain expression on T cells from old mice infected with *Mycobacterium tuberculosis*. *Experimental gerontology* 37.7 (2002): 907-916.
44. Shi, Ji., et al. PD-1 controls follicular T helper cell positioning and function. *Immunity* 49.2 (2018): 264-274.
45. Sage, P. T., et al. Defective TFH cell function and increased TFR cells contribute to defective antibody production in aging. *Cell reports* 12.2 (2015): 163-171.
46. Crotty, S. T follicular helper cell biology: A decade of discovery and diseases. *Immunity* 50.5 (2019): 1132-1148.
47. Bosco, M. J., et al. The exhausted $CD4^+$ $CXCR5^+$ T cells involve the pathogenesis of human tuberculosis disease. *International journal of infectious diseases* 74 (2018): 1-9.
48. Kumar, N. P., et al. Decreased frequencies of circulating $CD4^+$ T follicular helper cells associated with diminished plasma IL-21 in active pulmonary tuberculosis. *PLoS one* 9.10 (2014): e111098.
49. Simpson, N., et al. Expansion of circulating T cells resembling follicular helper T cells is a fixed phenotype that identifies a subset of severe systemic lupus erythematosus. *Arthritis & rheumatism* 62.1 (2010): 234-244.
50. Kudryavtsev, I., et al. Imbalance in B cell and T follicular helper cell subsets in pulmonary sarcoidosis. *Scientific reports* 10.1 (2020): 1059.
51. Boer, M. C., et al. KLRG1 and PD-1 expression are increased on T-cells following tuberculosis-treatment and identify cells with different proliferative capacities in BCG-vaccinated adults. *Tuberculosis* 97 (2016): 163-171.
52. Henao-Tamayo, M., et al. T lymphocyte surface expression of exhaustion markers as biomarkers of the efficacy of chemotherapy for tuberculosis. *Tuberculosis* 91.4 (2011): 308-313.
53. Lindenstrøm, T., et al. T cells primed by live mycobacteria versus a tuberculosis subunit vaccine exhibit distinct functional properties. *EBioMedicine* 27 (2018): 27-39.

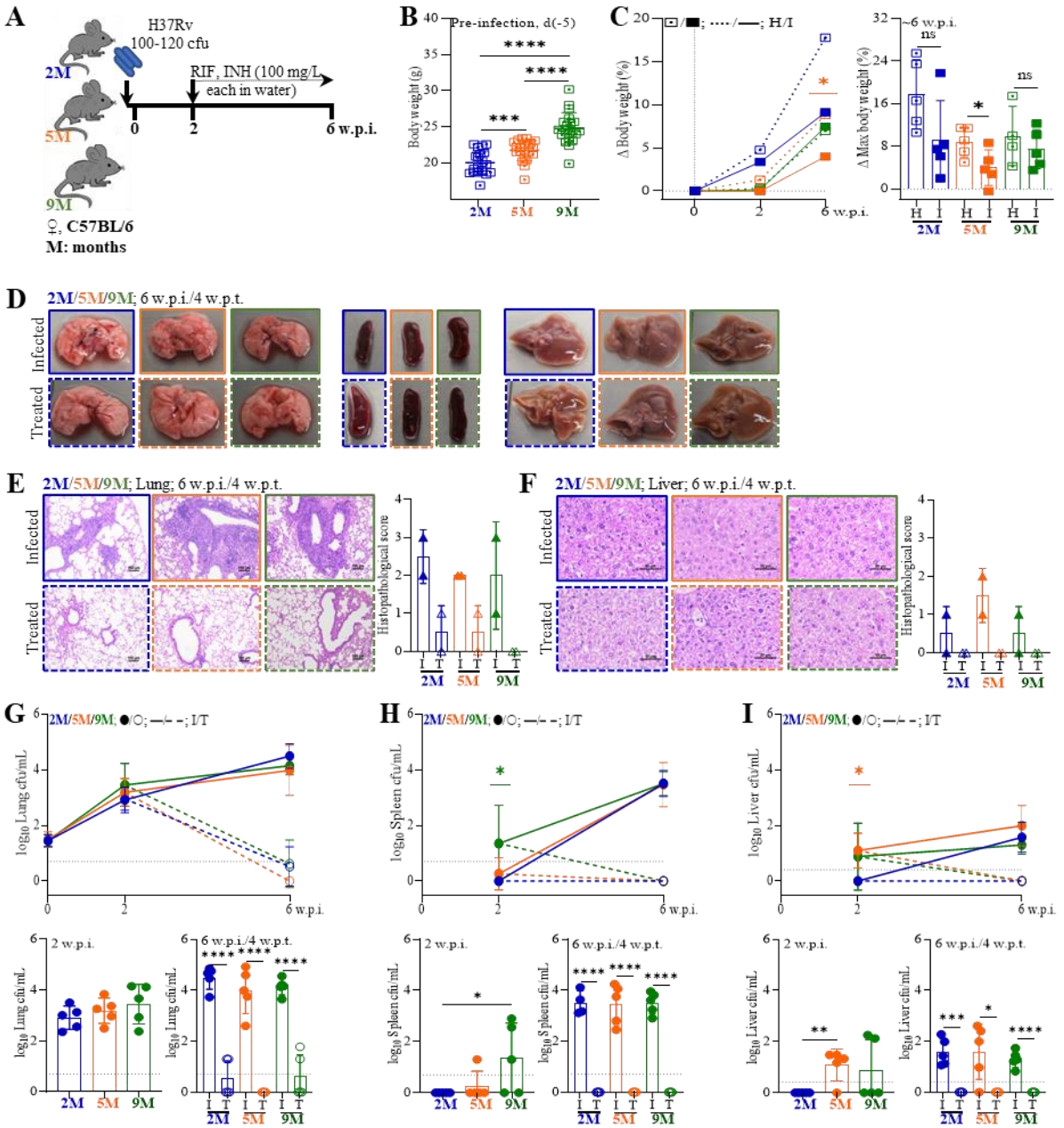

Figure 1. **Higher splenic Mycobacterial burden observed in *Mycobacterium tuberculosis* (Mtb) infected 9M C57BL/6 mice**. **A**. Schematic of the experimental details using C57BL/6 mice (female; age groups of 2, 5 and 9 months: M; 2M in blue, 5M in orange and 9M in green). **B**. Mice (n=20/age group) body weight (in gram) prior to infection (day -5). **C**. Changes in body weight and maximum body weight (%) of multiple mice age groups upon Mtb infection (healthy: H, ···· ; infected: I, —) are presented as mean of n=5 and individual mice respectively. **D**. Gross morphology of lung, spleen and liver from representative I group and rifampicin (RIF) and isoniazid (INH) treated group (T, - - -) at 6 w.p.i./4 w.p.t. of multiple age groups. **E**. Histopathological images (hematoxylin and eosin (H&E) stained slides) of lung (100× magnification, scale bar = 100 µm) and (**F**) liver (400×/50 µm) of mice of I and T groups at 6 w.p.i./4 w.p.t. of multiple age groups. The tissue histopathological scores (w.r.t. healthy, n = 2/age group/condition) are presented. Mycobacterial burden in the lung (**G**), spleen (**H**) and

liver (**I**) of mice belonging to I and T groups at 2 and 6 w.p.i./4 w.p.t. (treatment started at 2 w.p.i.). All bacterial load data points are a mean of n = 5/time point/age group/condition, with error bars (standard deviation). The individual data points at 2 w.p.i. and 6 w.p.i./4 w.p.t. are presented in the histograms. p-values: * ≤0.05, ** <0.005, *** <0.0005 ,**** <0.0001 at 95% confidence interval, ns: non-significant.

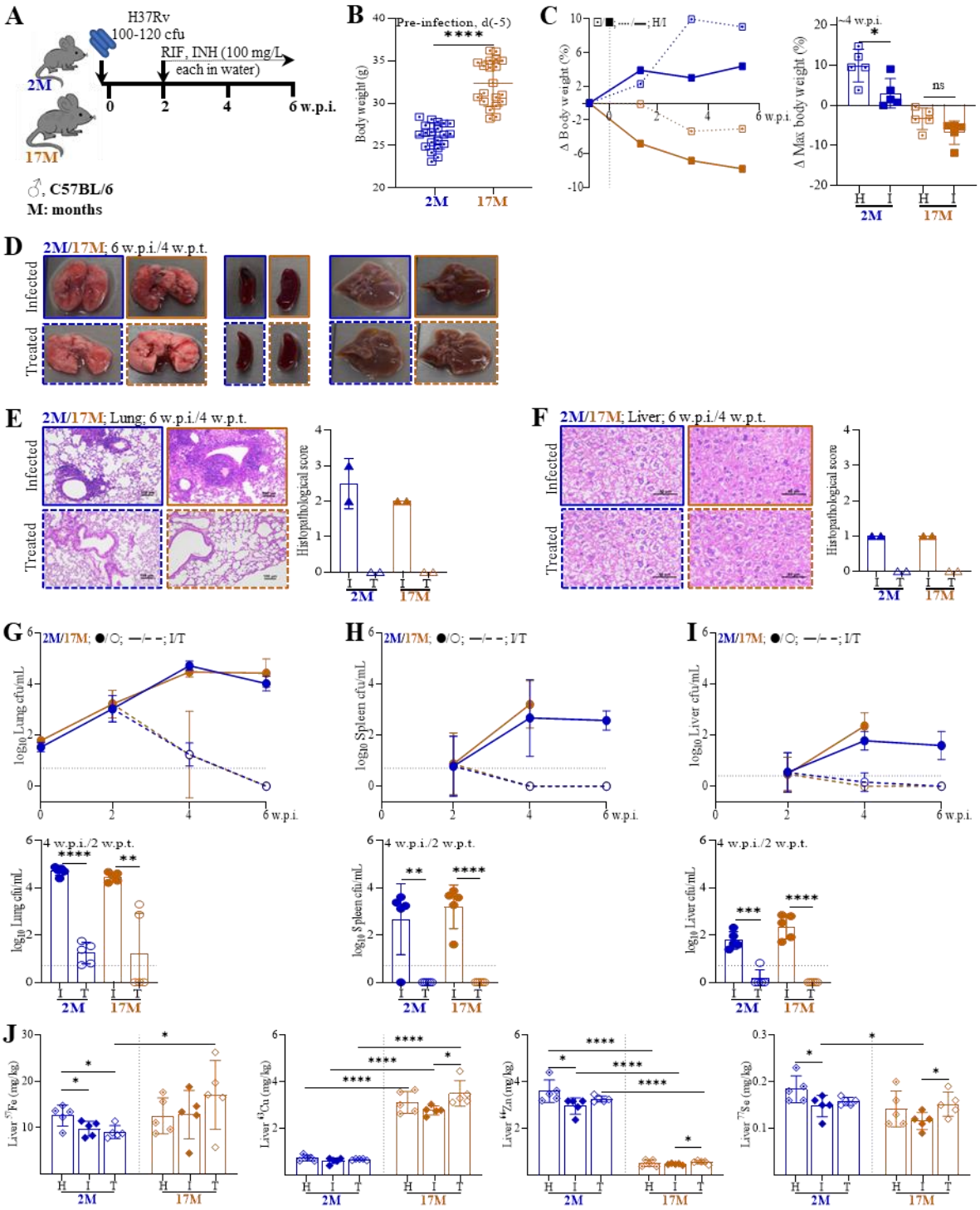

Figure 2. **Lungs of aged (17M) C57BL/6 mice receiving two weeks of rifampicin (RIF) and isoniazid (INH) treatment showed delayed clearance of *Mycobacterium tuberculosis* (Mtb)**. **A**. Schematic of the experimental details using C57BL/6 mice (male; age groups of 2 and 17 months: M; 2M in blue, and 17M in brown). **B**. Mice (n=20/age group) body weight (in gram) prior to infection (day -5). **C**. Changes in body weight and maximum body weight (%)

of 2M/17M groups upon Mtb infection (healthy: H, ···· ; infected: I, —) are presented as mean of n=5 and individual mice respectively. **D**. Gross morphology of lung, spleen and liver from representative I group and RIF and INH treated (T, −−−) group at 6 w.p.i./4 w.p.t. of 2M/17M groups. **E**. Histopathological images (hematoxylin and eosin (H&E) stained slides) of lung (100× magnification, scale bar = 100 μm) and (**F**) liver (400×/50 μm) of I and T groups at 6 w.p.i./4 w.p.t. of 2M/17M groups. The tissue histopathological scores (w.r.t. healthy, n = 2/age group/condition) are presented. Bacterial burden in the lung (**G**), spleen (**H**) and liver (**I**) of mice belonging to I and T groups at 2, 4 and 6 w.p.i./ 2 and 4 w.p.t. (treatment started at 2 w.p.i.). All bacterial load data points are a mean of n = 5/time point/age group/condition, with error bars (standard deviation). n=4 for 17M treated group at 4 w.p.t.. Data points for spleen and liver of infected 17M mice at 6 w.p.i. could not be recorded due to contamination in the plates. The individual data points at 4 w.p.i./2 w.p.t. are presented in the histograms. **J**. Abundance of liver micronutrients (in milligram per kilogram): iron (^{57}Fe), copper (^{63}Cu), zinc (^{66}Zn), selenium (^{77}Se) of I and T groups at 4 w.p.i./2 w.p.t. of 2M/17M groups. p-values: * ≤0.05, ** <0.005, *** <0.0005 ,**** <0.0001 at 95% confidence interval, ns: non-significant.

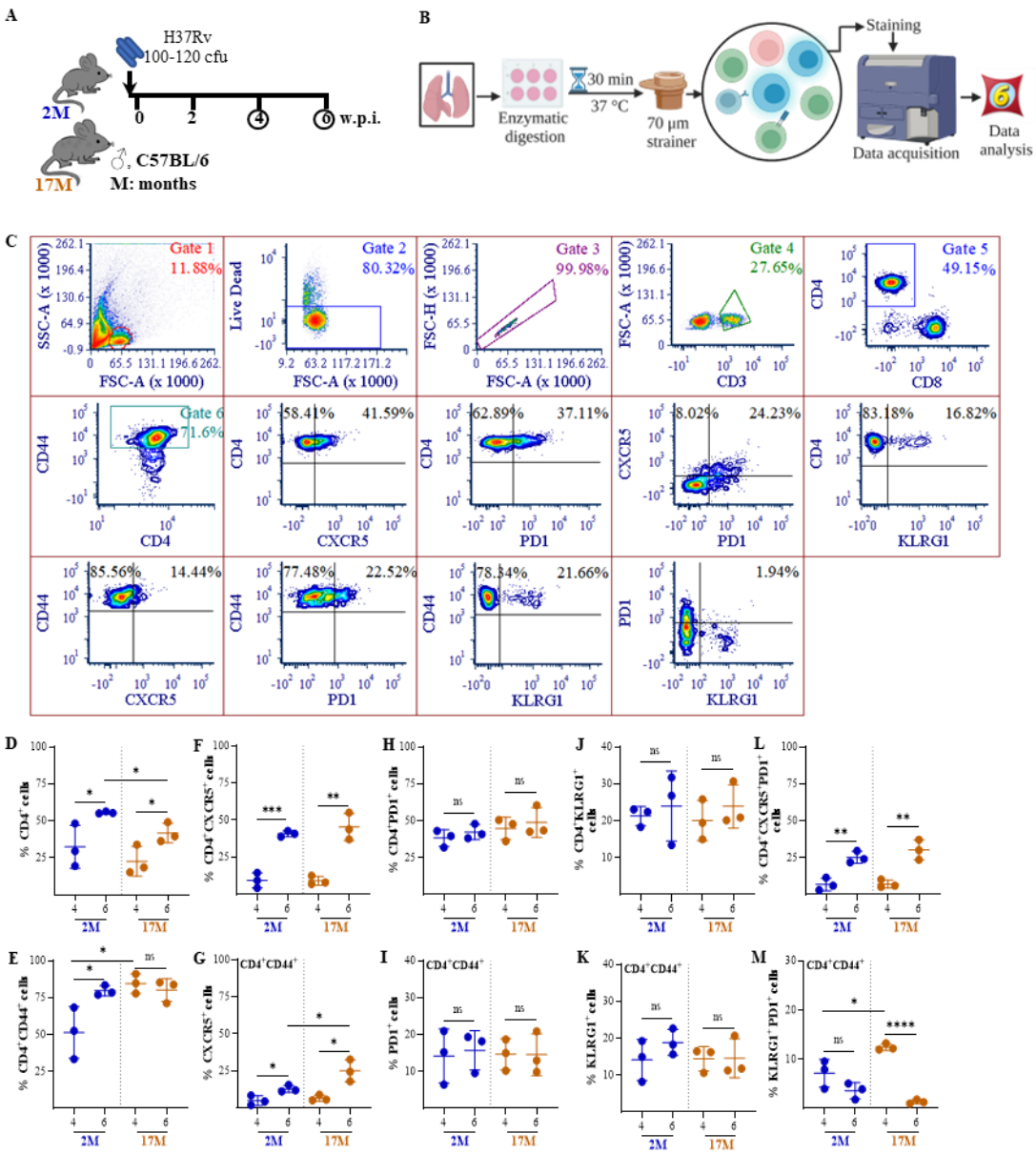

Figure 3. **Lung CD4⁺CD44⁺KLRG1⁺PD1⁺ cells declined in *Mycobacterium tuberculosis* (Mtb) infected aged (17M) C57BL/6 mice**. **A**. Schematic showing Mtb infection of C57BL/6 mice of two age groups (2 and 17 in months; M; 2M in blue and 17M in brown). **B**. Method adopted for lung immune cell isolation, flow cytometry data acquisition and data analysis. **C**. Representative gating strategy followed to monitor the lung T cell frequencies of Mtb infected mice at 4 and 6 w.p.i.. Frequency of individual T cell subsets are presented in (**D**) $CD4^+$, (**E**) $CD4^+CD44^+$, (**F**) $CD4^+CXCR5^+$, (**G**) $CD4^+CD44^+CXCR5^+$, (**H**) $CD4^+PD1^+$, (**I**) $CD4^+CD44^+PD1^+$, (**J**) $CD4^+KLRG1^+$, (**K**) $CD4^+CD44^+KLRG1^+$, (**L**) $CD4^+CXCR5^+PD1^+$, and (**M**) $CD4^+CD44^+KLRG1^+PD1^+$. n = 3/time point/age group; p-values: * ≤0.05, ** <0.005, *** <0.0005, **** <0.0001 at 95% confidence interval, ns: non-significant.

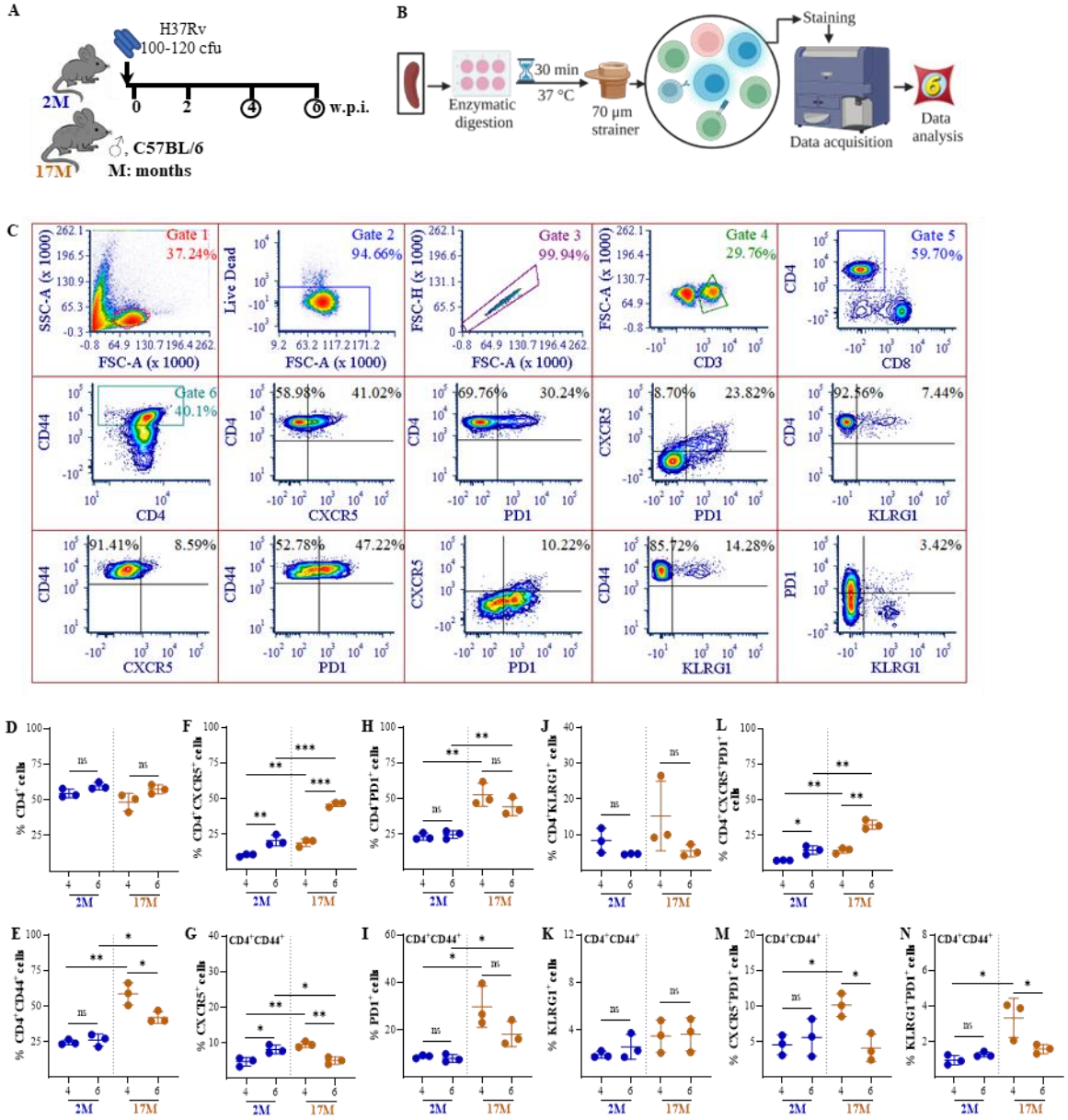

Figure 4. **Splenic CD4$^+$CD44$^+$CXCR5$^+$PD1$^+$ cell frequency declined in *Mycobacterium tuberculosis* (Mtb) infected aged (17M) C57BL/6 mice**. **A**. Schematic showing Mtb infection of C57BL/6 mice of two age groups (2 and 17 in months; M; 2M in blue and 17M in brown). **B**. Method adopted for lung immune cell isolation, flow cytometry data acquisition and data analysis. **C**. Representative gating strategy followed to monitor the splenic T cell frequencies of Mtb infected mice at 4 and 6 w.p.i.. Frequency of individual T cell subsets are presented in (**D**) CD4$^+$, (**E**) CD4$^+$CD44$^+$, (**F**) CD4$^+$CXCR5$^+$, (**G**) CD4$^+$CD44$^+$CXCR5$^+$, (**H**) CD4$^+$PD1$^+$, (**I**) CD4$^+$CD44$^+$PD1$^+$, (**J**) CD4$^+$KLRG1$^+$, (**K**) CD4$^+$CD44$^+$KLRG1$^+$, (**L**) CD4$^+$CXCR5$^+$PD1$^+$, (**M**) CD4$^+$CD44$^+$CXCR5$^+$PD1$^+$, and (**N**) CD4$^+$CD44$^+$KLRG1$^+$PD1$^+$. n = 3/time point/age group; p-values: * ≤0.05, ** <0.005, *** <0.0005 at 95% confidence interval, ns: non-significant.

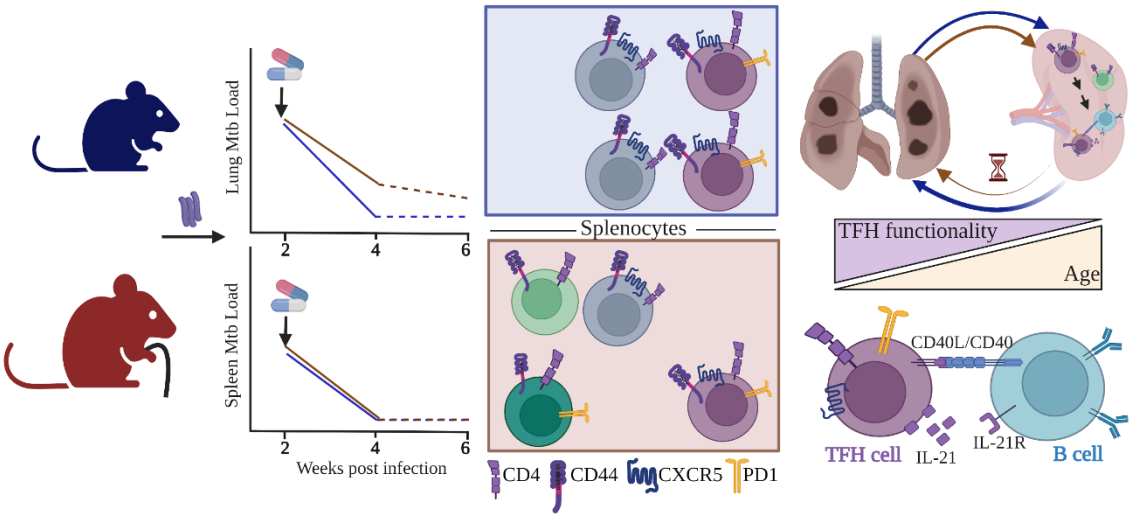

Figure 5. Aged (17M) C57BL/6 mice showed delayed lung *Mycobacterium tuberculosis* clearance upon rifampicin and isoniazid treatment with low splenic T-follicular helper cells (TFH) than controls (2M).